

Ultra-high energy cosmic rays: are they isotropic?

Gustavo Medina-Tanco

Institute of Astronomy and Geophysics, University of Sao Paulo, Sao Paulo, Brasil

gustavo@iagusp.usp.br

Abstract

From the analysis of AGASA data above 4×10^{19} eV, we show that the ultra-high energy cosmic rays flux is neither purely isotropic, nor reflects the expected anisotropy from a pure source distribution that maps large scale structure in the local universe. The arrival distribution seems to be the result of a mixture of fluxes (e.g., dark matter halo plus large scale structure) or the superposition of a direct and a diffuse radiation field components respectively. Another viable option is an arbitrary extragalactic flux reprocessed by a magnetized galactic wind model as recently proposed in the literature.

Subject headings: cosmology: dark matter — cosmology: large-scale structure of universe — Galaxy: halo — galaxies: magnetic fields — ISM: cosmic rays — ISM: magnetic fields

I. INTRODUCTION

As ultra high energy cosmic rays (UHECR) continue to puzzle physicists and astronomers alike, the basic question of the isotropy of the flux beyond the unobserved GZK cut-off [1,2] retains a high priority. A recent analysis by the AGASA group [3] shows a trend towards isotropy at the highest energies, although some clusters of events (3 doublets and a triplet)

are identified with a very low chance probability. This seeming contradiction is still more disturbing as both, bottom-up and top-down production mechanisms generally produce anisotropy to some degree in a natural way. In the present letter, we address the problem of isotropy of supra-GZK cosmic rays ($E > 4 \times 10^{19}$ eV) by using propagation simulations and one- and two-dimensional tests over simulated and existing world data (mainly from AGASA). The significance of the clusters of events detected by AGASA is also discussed in different scenarios.

II. NUMERICAL METHOD AND RESULTS

Probably the conceptually simplest production models of UHECR are the ones involving bottom-up mechanisms. All of them, require that the sources of the particles group in more or less the same way as luminous matter does. Furthermore, on large scales, luminous matter trace roughly the distribution of cold dark matter (DM), although bias factors have to be taken into account. DM is involved in most of the top-down production mechanisms. It is therefore important to check the expected signature from such a source distribution (which we will call the LLMD - local luminous matter distribution - scenario).

We use a numerical simulation approach to track UHECR propagation through the intergalactic medium and evaluate their arrival distribution. The actual distribution of galaxies is used for the UHECR sources nearer than 100 Mpc [4]. Additionally, the same procedure as in [6,5] is used in the description of the intergalactic magnetic field (IGMF): a cell-like spatial structure, with cell size given by the correlation length, $L_c \propto B_{IGMF}^{-2}(r)$. The intensity of the IGMF, in turn, scales with luminous matter density, ρ_{gal} as $B_{IGMF} \propto \rho_{gal}^{0.3}(r)$ [7] and the observed IGMF value at the Virgo cluster ($\sim 10^{-7}$ G, [8]) is used as the normalization condition. Note, however, that the IGMF could be ordered and coherent on large scales [9], in which case the propagation of UHECR should be strongly model dependent [10]. Test particles (protons) are injected at the sources with a spectrum $dN/dE \propto E^{-2}$ ($E < 10^{24}$ eV) and propagated through the intergalactic magnetic field up to the detector

on Earth. Energy losses due to redshift, pair production and photo-pion production due to interactions with the cosmic microwave background radiation (CMBR) are also included.

The Aitoff projection of the resultant (2D) arrival probability density is shown in Figure 1 in galactic coordinates. The mask covers the plane of the galaxy, where the actual distribution of galaxies is not well known due to obscuration by dust. The curved, thick line is the celestial equator. Superimposed on the figure are the available events with $E > 4 \times 10^{19}$ eV observed by AGASA (47 events [3]), Haverah Park (27 [11]), Yakutsk (24 [12]) and Volcano Ranch (6 [13]). The arrival probability contours trace quite well the local large scale structures. The supergalactic plane (SGP), in particular, can be easily distinguished running from North to South approximately along the $l = 135$ galactic meridian. It is apparent from the figure that, despite some conspicuous clusters in the vicinity of the SGP, the actual observed distribution of UHECR is much more isotropic than what one would expect if their sources aggregate like the luminous matter. Unfortunately, given the non-uniform exposure in declination of the various experiments and the low number statistics involved, it is not trivial to quantify this statement.

The view of the AGASA group [3] is that supra-GZK events arrive isotropically at Earth. Nevertheless, to complicate things further, three doublets and a triplet within a separation angle of 2.5° are also observed.

Independent tests are applied in order to confront AGASA data, at the same level of statistical significance, with two opposite yet plausible scenarios: a completely isotropic UHECR flux and a flux originated from sources that spatially map the large scale distribution of matter inside the GZK-sphere.

Two pools of particles, with 20 million protons each, were constructed: one strictly isotropic, the other obtained from the simulation results depicted in Figure 1. Independent samples are extracted from these reservoirs using the response in declination of the exposure of the AGASA experiment as a selection criteria [14]. The size of each individual sample is equal to the number of events (47) actually observed by AGASA above 4×10^{19} eV.

The most elemental analysis that can be made regarding isotropy is one-dimensional,

in right ascension (RA), where other complicating factors like non-uniform exposure in declination and low number statistics are more easily dealt with. Figures 2a and 2b show different forms of visualizing the distribution of events in RA. The shaded bands (figure 2a) in the background correspond to the 68% and 95% confidence levels of the expected distribution of events in RA for a sample of size 47 protons originated in the LLMD scenario. Despite the small size of the samples some features are clearly seen. The largest peak is the signal from the Virgo-Coma line of sight towards the North galactic pole. The opposite half of the SGP (towards the second quadrant in galactic latitude) is responsible for the smaller peak around 30° . The deep depressions surrounding the Virgo peak correspond to the Orion (left) and Local (right) voids, the most prominent structures in our immediate neighborhood, combined with the spurious effect of obscuration of the galaxy distribution due to the galactic plane.

The thick continuous lines in the same figure, correspond to the 68% and 95% confidence levels of the distribution in RA when the incident UHECR flux is isotropic. We can see that, even with so few events, both limits should be distinguishable.

The heavy squares represent the AGASA data (same bin size as for the models above) and are consistent with an isotropic distribution. No signature is seen from the Virgo peak and, furthermore, the most populated bins fall in a region corresponding to the Local Void.

A more quantitative treatment to characterize the anisotropy in RA is the first harmonic analysis [15]. Thus, given a data sample, the amplitude $r_{1h} = \sqrt{a_{1h}^2 + b_{1h}^2}$ and phase $\Psi_{1h} = \tan^{-1}(b_{1h}/a_{1h})$ are calculated, where $a_{1h} = \frac{2}{N} \sum_{i=1}^N \cos \alpha_i$, $b_{1h} = \frac{2}{N} \sum_{i=1}^N \sin \alpha_i$ and α_i is the right ascension of an individual event.

r_{1h} and Ψ_{1h} are calculated for 10^3 samples drawn from the isotropic and anisotropic (LLMD) distributions and the results are shown in figure 2b with small dots and crosses respectively. Both cases are very well discriminated in the r_{1h} - Ψ_{1h} plane. The error box for the first harmonic of AGASA data (calculated by [16]) is also displayed (hatched region), and is completely consistent with an isotropic UHECR flux. Moreover, the AGASA result by itself, seems completely inconsistent with the LLMD scenario. However, when the phase and

amplitudes obtained from other major experiments are considered (large, thick horizontal bars in Figure 2b for Haverah Park -HP- Volcano Ranch -VR- Yakutsk -YK; see [16]) the picture looks suggestively different, since all the phase observations are clustered inside the same quadrant in RA, covering the right wing of the Virgo peak. That is, despite the fact that every isolated measurement is consistent with isotropy, the observed phases seem to show a systematic enhancement in the direction of the interface between the SGP and the large adjacent Local void. It must also be noted that Haverah Park and Volcano Ranch data behave more like a transition between the isotropic and LLMD scenarios. Three out of four first harmonic phases (HP, YK and VR) include the North galactic pole within one S.D. level, while the forth (AGASA) include it within two S.D.. The exclusion of the observed UHECR events inside the obscuration band, $b < 10^\circ$, changes the phase of the AGASA result by only 6° (from 258° to 252°) and, therefore, previous conclusions are unchanged by this effect.

Clearly, a two-dimensional analysis of the data would be highly desirable in order to answer questions as simple as whether the data is isotropic or unimodal. One way of doing this, given the small number of events involved and the non-uniformity of the distribution of events in declination due to experimental limitations, is to analyze the normalized eigenvalues τ_1 , τ_2 and τ_3 of the orientation matrix \mathbf{T} of the data. Defining $\mathbf{T}_{i,j} = \sum_{k=1}^N \mathbf{v}_i^k \mathbf{v}_j^k$, where \mathbf{v}^k are the N unit vectors representing the data over the celestial sphere and assuming $0 \leq \tau_1 \leq \tau_2 \leq \tau_3 \leq 1$, the shape, $\gamma = \log_{10}(\tau_3/\tau_2)/\log_{10}(\tau_2/\tau_1)$, and the strength parameter, $\zeta = \log_{10}(\tau_3/\tau_1)$, can be built [17]. The shape criterion γ is useful in discriminating girdle-type distributions from clustered distributions. The larger the value of γ more clustered is the distribution. Uniform, nearly isotropic, distributions have $\zeta \sim 0$. Because of the nature of the experimental setup, the observed distribution of UHECR is girdle in nature, regardless of the isotropicity of the UHECR flux. Therefore, in figure 3 we compare the results for 10^3 isotropic (rhombes) and LLMD (circles) samples respectively with the AGASA sample in the γ - ζ plane. It can be seen that the isotropic and LLMD scenarios should be very well separated with the available data, albeit its smallness. AGASA data (thick cross), on the

other hand, does not fit either of these scenarios, being an intermediate case.

Figure 4 shows the number of doublets with separation smaller than 2.5° obtained from 10^4 samples of 47 events each, drawn from isotropic and LLMD populations. AGASA observed 3 pairs, which is a large number (8% chance probability) for an isotropic UHECR flux, and a rather small number (but still inside the 68% C.L. at 13% probability) if compared with the average value of 5.5 pairs obtained for the anisotropic flux. The situation is analogous for triplets. One triplet was actually observed by AGASA, while 1.3 ± 3.1 is expected for the LLMD model and 0.02 ± 0.2 for the isotropic model. It should also be noted that the AGASA triplet C2 and pair C1 (actually a triplet if Haverah Park data is included), as well as the lower energy cluster BC2 fall on the SGP, on top of a maximum of the arrival probability [5], strengthening the case for an extragalactic origin inside this structure.

III. DISCUSSION AND IMPLICATIONS

Different tests have been applied to the analysis of the isotropy of UHECR with $E > 4 \times 10^{19}$ eV. Test samples are drawn from both, an isotropic flux of particles and an anisotropic flux originated in sources with the local luminous matter distribution. Samples used to compare with AGASA data have a size of 47 events and are selected according to the same declination sensitivity as AGASA's. Our results can be summarized as follows:

1) The comparison between arrival directions of the UHECR above 4×10^{19} eV and the expected arrival probability density, calculated under the assumption of UHECR sources that cluster as the luminous matter in the nearby universe, shows a remarkable degree of isotropy, despite a notorious tendency for clusters to appear on top of large scale structure signatures (Fig.1).

2) AGASA's RA distribution is consistent with an isotropic distribution (Fig.2).

3) 10^4 simulated experiments equivalent to AGASA show that a set as small as 47 UHECR is enough to separate extremely well isotropic and LLMD scenarios in the

amplitude-phase plane; AGASA's error box is completely consistent with isotropy and inconsistent with LLMD (Fig.2)

4) Nevertheless, the phases of HP, VR, YK and AGASA fall in the same quadrant in phase (Fig.2), which covers the interface between the SGP in the general Virgo direction and the adjacent Local void. The first three experiments include the North galactic pole inside 1 SD, and AGASA at 2 SD.

5) The comparison of AGASA data with 10^4 simulated data sets from isotropic and LLMD fluxes on the γ - ζ (shape-strength) plane show that the former is an intermediate case, more clustered than isotropic samples but less than LLMD (Fig.3).

6) The number of pairs observed by AGASA is too large for an isotropic flux, but it is within the 68% CL for LLMD flux (Fig.4).

While a first order interpretation of the AGASA data certainly points to an isotropic flux of UHECR, consideration of the first harmonic analysis of other data sets and of two-dimensional tests over the AGASA data itself, as well as expected numbers of doublets for isotropic and anisotropic samples, point to a more complicated, intermediate picture with a certain degree of mixture of both limiting cases.

We can envisage at least three scenarios in which such a result could be obtained:

1) The sources involve bottom-up mechanisms associated with luminous matter but some of the events are scattered in the intergalactic medium such that we observe the composition of a diffuse and a direct component [18].

2) The sources involve bottom-up mechanisms associated with luminous matter but there is a large local magnetic structure, like a magnetized galactic wind, which isotropize the UHECR flux upon traversing the galactic halo [19]. As the energy of the particles increases, and as long as they all have the same mass, the degree of isotropization should decrease making the galactic pole visible.

3) The sources involve top-down mechanisms associated with dark matter whose distribution roughly associates with the LLMD. In this case, the observed flux is the composition of an extragalactic component, whose signature is not very different from that of the LLMD,

and a component originated in the halo of our own galaxy. [20] showed that, under general conditions, the halo component would dominate the extragalactic flux by at least two orders of magnitude. This is only true, however, in the unrealistic case of dark matter uniformly distributed in intergalactic space. Nevertheless, dark matter aggregates strongly and tends to be overabundant, by factors of $\sim 10^2$, in the center of galaxy clusters when compared to its abundance in the halos of isolated galaxies. It can therefore be shown that, in a sample of 47 events, and assuming Virgo as the only source of extragalactic events, 3-7 events should originate in Virgo and arrive inside a solid angle of approximately the size of the cluster. This could give rise to a slight anisotropy that correlates with the SGP when combined with the almost isotropic flux originated in a large galactic halo. Note, however, that the solid angle does not need to point exactly in the direction of Virgo, depending on the large scale structure of the intervening magnetic field.

Obviously, more high quality, high energy data from HiRes and Auger are badly needed.

Acknowledgments. The author benefited from discussions with Alan. A. Watson, Peter Biermann, Todor Stanev, Eun-Joo Ahn and Torsten Ensslin. This work is partially supported by the Brazilian agencies FAPESP and CNPq.

REFERENCES

- [1] K. Greisen. *Phys. Rev. Lett.* **16**: 748, (1966). G. T. Zatsepin & V. A. Kuzmin. *Sov. Phys.-JETP Lett.* **4**: 78, (1966)
- [2] M. Takeda et al. *Phys. Rev. Lett.* **81**: 1163, (1998).
- [3] M. Takeda et al. *Astrophys.J.* **522**: 225 (1999), astro-ph/9902239.
- [4] Huchra, J. Geller, M., Clemens, C., Tokarz, S and Michel, A. 1992, Bull. C.D.S. **41**, 31. Version June 1998 of ZCAT.
- [5] Medina Tanco G. A. *Ap. J. Letters* **495** L71 (1998).
- [6] Medina Tanco, G. A. *25th ICRC* **4** 477 (1997).
- [7] Vallée J. P. *Fundamental of Cosmic Phys.* **19** 1 (1997).
- [8] Arp, H. *Phys. Lett. A* **129** 135 (1988).
- [9] Ryu D., Kang H. and Biermann P. L. *A.&A.* **335** 19 (1998).
- [10] Medina Tanco G. A. *Ap. J. Letters* **505** L79 (1998).
- [11] Reid, R. J. O. and Watson, A. A, 1980, Catalogue of Highest Energy Cosmic Rays (ed. M Wada) WDC C2 for CR, IPCR, Tokyo, Vol. 1, pp 61.
- [12] Afanasiev, B.N. et al., 1995, Proceedings of 24th International Cosmic Ray Conference (Roma) **2**, 796.
- [13] Linsley, J, 1980, Catalogue of Highest Energy Cosmic Rays (ed. M. Wada) WDC C2 for CR, IPCR, Tokyo, Vol. 1 pp 1.
- [14] Uchihori, Y, et al. *Proc. of Int.Symp. on Extremely High Energy Cosmic Rays ICRR*, Univ. of Tokyo (ed. M. Nagano), p 50 (1997).
- [15] Linsley J. *Phys. Rev. Lett.* **34** 1530 (1975).

- [16] Medina Tanco G. A. and Watson A. A. *Astropart. Phys.* **12** 25 (1999).
- [17] Fisher N. I., Lewis T. and Embleton B. J. J. *Statistical analysis of spherical data*, Cambridge Univ. Press., Cambridge (1993).
- [18] Enßlin T.A., 1999, ‘Radio Ghosts’ in Ringberg Workshop on ‘Diffuse Thermal and Relativistic Plasma in Galaxy Clusters’, Eds: H. Böhringer, L. Feretti, P. Schuecker, MPE Report No. 271, 1999, 275, astro-ph/9906212; Medina Tanco G. A. and Enßlin T. A. in preparation
- [19] Ahn E.J., Medina Tanco G.A., Biermann P. and Stanev T. *Phys.Rev.Lett.* submitted, astro-ph/9911123
- [20] Dubovsky S.L., Tinyakov P.G., astro-ph/9802382.

FIGURES

FIG. 1. Arrival probability distribution for the LLMD model (contour lines in the background) compared with the actual published data above 4×10^{19} eV from AGASA, Haverah Park, Yakutsk and Volcano Ranch.

FIG. 2. (a) Arrival directions (right ascension) of UHECR above 4×10^{19} eV for the LLMD (hatched regions) and isotropic (lines) models, as well as the observed AGASA data (squares). 68% and 95% confidence levels are shown for both models. Confidence levels are calculated for each individual bin after 1000 independent experiments (with 47 events each - same number as the AGASA sample) were performed. (b) Amplitude and phase of the first harmonic calculated for 10^3 samples drawn from the isotropic (circles) and anisotropic (LLMD - crosses) distributions. The size of individual samples is 47 protons, as in AGASA. The hatched region is the (1σ) error box calculated from AGASA observations, while the thick horizontal bars are the 1σ error bars for the phases of Volcano ranch, Haverah Park and Yakutsk experiments. In both cases, (a) and (b), samples are selected with the same declination distribution expected for the AGASA experiment.

FIG. 3. Two-dimensional eigenvector analysis (see the text for the definition of the shape and strength parameters). The heavy cross is the AGASA observation. Rhombuses and circles correspond to isotropic and LLMD simulations respectively.

FIG. 4. Expected frequency of doublets for the isotropic (crosses) and LLMD (rhombuses) models respectively. The horizontal bars show the expected mean and one standard deviation intervals for each model.

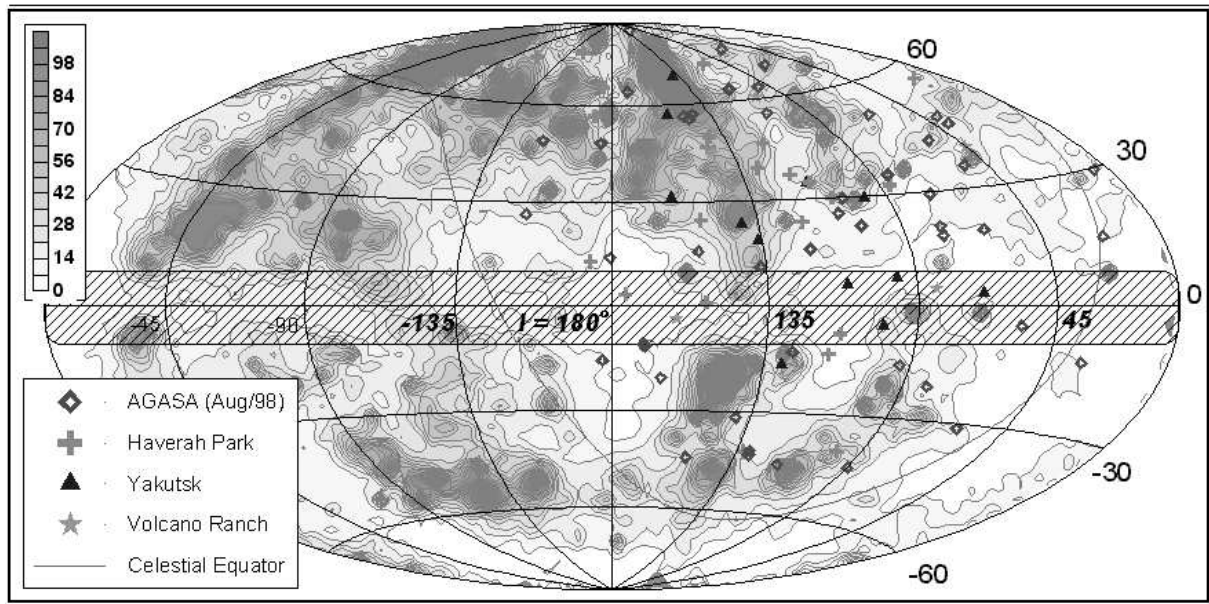


Figure 1

G. A. Medina Tanco- Ultra-high energy...

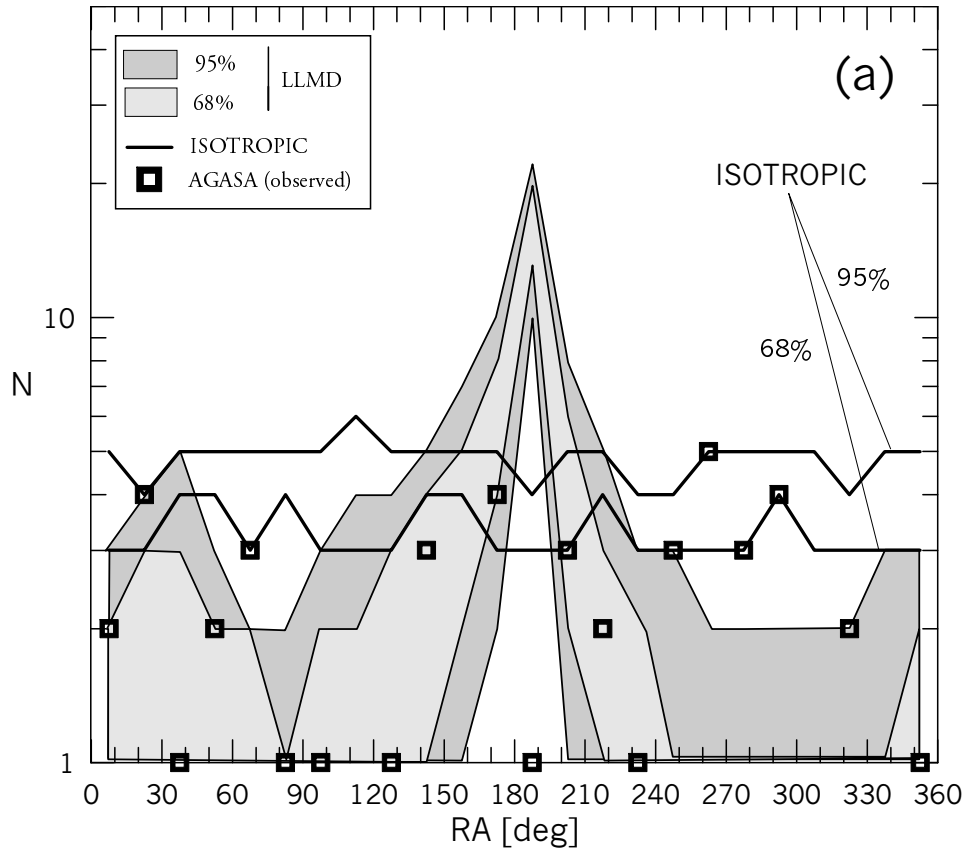


Figure 2a

G. A. Medina Tanco- Ultra-high energy...

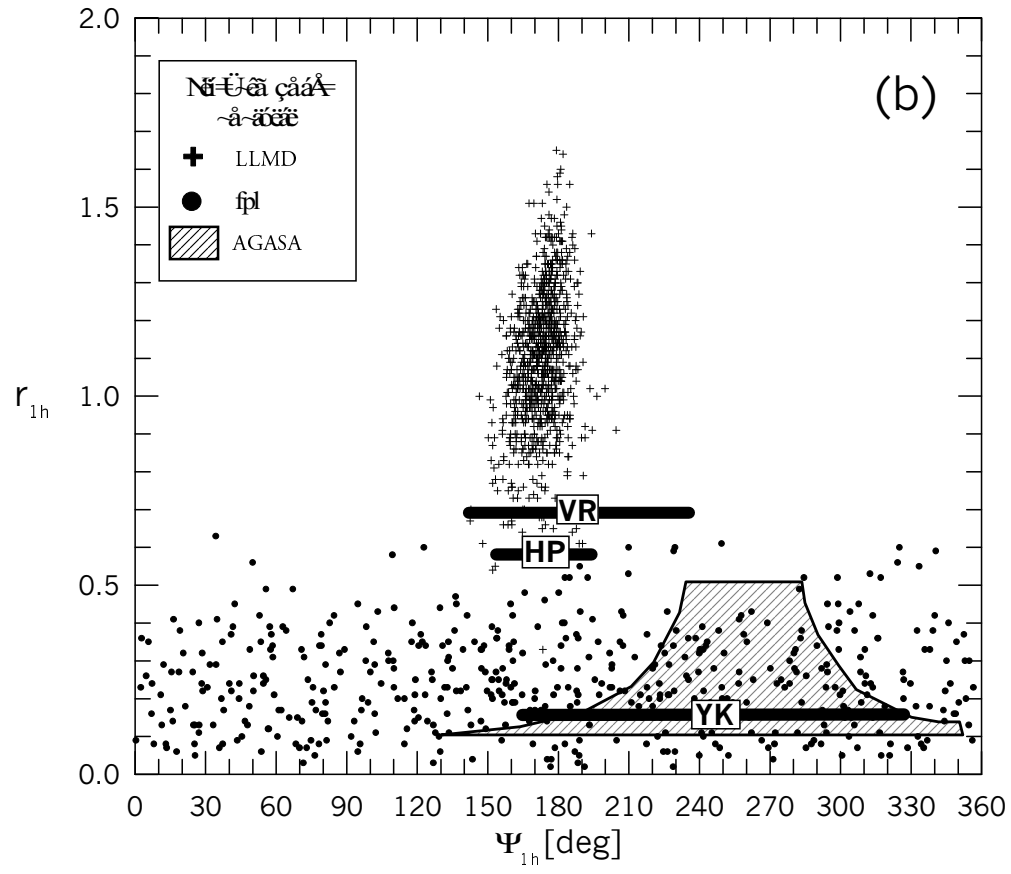


Figure 2b

G. A. Medina Tanco- Ultra-high energy...

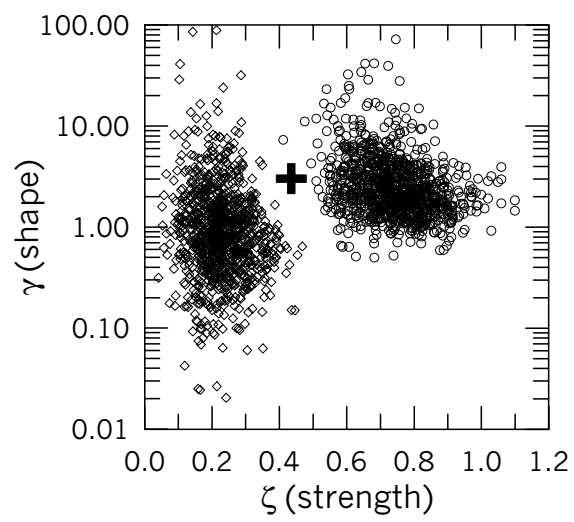


Figure 3

G. A. Medina Tanco- Ultra-high energy...

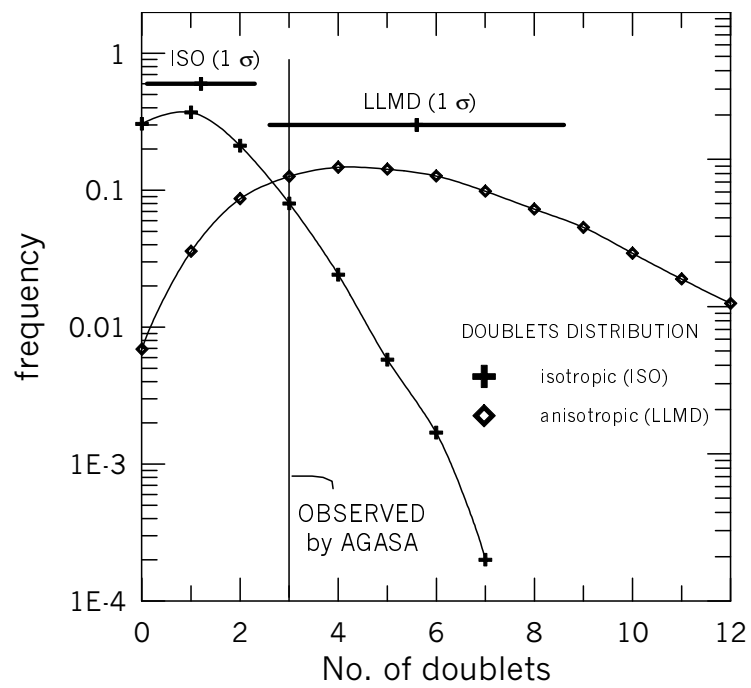


Figure 4

G. A. Medina Tanco- Ultra-high energy...